horticulturae

MDPI

Article

Identification of Laccase Genes in Grapevine and Their Roles in Response to *Botrytis cinerea*

Ran Wan [1,2,†], Zhenfeng Yang [1,2,†], Jun Liu [1,2], Mengxi Zhang [1,2], Jian Jiao [1,2], Miaomiao Wang [1,2], Kunxi Zhang [1,2], Pengbo Hao [1,2], Yu Liu [1,2], Tuanhui Bai [1,2], Chunhui Song [1,2], Shangwei Song [1,2], Jiangli Shi [1,2,*] and Xianbo Zheng [1,2,*]

[1] College of Horticulture, Henan Agricultural University, Zhengzhou 450002, China; wanxayl@henau.edu.cn (R.W.); yzf15038898023@163.com (Z.Y.); lj13550345839@163.com (J.L.); zmx18337011095@126.com (M.Z.); jiaojian@henau.edu.cn (J.J.); wmm2018@henau.edu.cn (M.W.); kunxi66@163.com (K.Z.); hao_pb@henau.edu.cn (P.H.); yuliu@henau.edu.cn (Y.L.); tuanhuibai@henau.edu.cn (T.B.); songchunhui060305@henau.edu.cn (C.S.); songsw@henau.edu.cn (S.S.)

[2] Henan Key Laboratory of Fruit and Cucurbit Biology, College of Horticulture, Henan Agricultural University, Zhengzhou 450002, China

* Correspondence: sjli30@henau.edu.cn (J.S.); xbzheng@henau.edu.cn (X.Z.)

† These authors contributed equally to this work.

Abstract: Laccases are the key enzymes responsible for plant lignin biosynthesis and responses to environment stress. However, the roles of LAC genes in plant disease resistance are still largely unknown, especially in grapevine, one of the most important horticultural crops in the world. Its quality and yield are very vulnerable to gray mold disease caused by *Botrytis cinerea*. In total, 30 *VvLAC* genes were identified and found to be unevenly distributed on seven chromosomes; they were classified into seven groups based on phylogenetic analysis according to the criteria applied in *Arabidopsis thaliana*. Collinearity and synteny analyses identified some orthologous gene pairs in Vitis vinifera and a few paralogous gene pairs among grape and peach. The *VvLAC* gene family has diverse gene structures and a highly conserved motif composition. The prominent presence of the MYB cis-elements in each *VvLAC* promoter highlighted MYB transcriptional factors as the main regulators of *VvLAC* genes. Furthermore, twenty-five *VvLAC* genes with functional redundancy are probably implicated in grape lignin biosynthesis. The expression patterns of the *LAC* genes in grape leaves of Chinese wild *V. amurensis* 'Shuangyou' (SY), a germplasm highly resistant to *B. cinerea*, were investigated through transcriptomic data and qRT-PCR verification. Combined with the phylogenetic analysis, with *AtLACs* participating in lignin metabolism, and the cis-element analysis, *VaLAC14*, *VaLAC19*, *VaLAC24* and *VaLAC30* were identified as key candidate genes for lignin biosynthesis in the grape response to *B. cinerea*. This study supplies a comprehensive understanding of the classification, evolution, structure and responses of the grape LAC genes against *B. cinerea*. It also provides valuable genetic resources for functional characterization towards enhancing grapevine disease resistance.

Keywords: grape laccase and lignin; the *VvLAC* gene family; gene expression; response to *Botrytis cinerea*

Citation: Wan, R.; Yang, Z.; Liu, J.; Zhang, M.; Jiao, J.; Wang, M.; Zhang, K.; Hao, P.; Liu, Y.; Bai, T.; et al. Identification of Laccase Genes in Grapevine and Their Roles in Response to *Botrytis cinerea*. *Horticulturae* **2024**, *10*, 376. https://doi.org/10.3390/horticulturae10040376

Academic Editor: Francesco Faretra

Received: 24 February 2024
Revised: 24 March 2024
Accepted: 3 April 2024
Published: 9 April 2024

1. Introduction

Grape is an important fruit crop worldwide with huge economic value. With the increase in grape planting years, the base number of pathogenic seedlings and insect population is gradually increasing [1]. The occurrence of *Botrytis cinerea* on grape, the ubiquitous necrotrophic fungal pathogen, is becoming more and more serious, resulting in a prominent problem of yield and quality decline [1,2]. *B. cinerea* causes serious damage to young leaves, young tendril, flower buds and ripened fruit of grape; it is generally called gray mold and is the second most important plant disease in the world [1–4].

B. cinerea has a very powerful 'arsenal' for causing disease in more than 1000 plant species which is especially characterized by massive secretion of cell wall degrading en-

zymes, such as BcPGs (endo-polygalacturonase), BcPMEs (pectin methylesterase), BcCBHs (cellobiohydrolase) and so on, as one of the primary infection strategies [5–7]. The cell wall matrix is one of the first and largest plant structures that pathogens encounter when interacting with potential hosts [8]. Lignin is one of the main components of the plant cell wall, and as a complex phenolic polymer produced by the phenylalanine/tyrosine metabolic pathway, it plays important roles in plant defense by enhancing plant cell wall rigidity, protecting cell wall integrity, acting as phytoalexins and acting as a physical barrier [9–11]. Previous studies have revealed that the cell wall strengthening through lignin accumulation mediated by the ethylene- and abscisic acid-associated pathways is significantly involved in the plant response to *B. cinerea* [12,13]. Lignin biosynthesis was also observed in grapevine defense against trunk diseases, downy mildew, Pierce's disease and postharvest infections [14–16]. Particularly, grapevine resistance to *B. cinerea* is also suggested to be associated with lignin metabolism. Higher lignin content was detected in Greek grape berries of the highly resistant 'Limnio' variety than in those of the susceptible 'Roditis' variety [17]. The genes associated with grapevine lignin resistant against *B. cinerea* remain unexplored.

In recent years, laccases (LACs), as one of the classes of key enzymes, have been found to have the important function of polymerizing lignin monomers into lignin in the cell wall [9,18]. A total of 17 laccase genes have been identified in *Arabidopsis thaliana,* and among them, *AtLAC4*, *AtLAC17*, *AtLAC2* and *AtLAC15* have been shown to participate in lignin polymerization in leaves, seed coat and roots [19–23]. The expression of *AtLAC4* and *AtLAC17* contributes to constitutive lignification in stems and to lignin monomer deposition in fibers; the *lac4 lac17* mutant increases their monolignol glucosides and display dwarfism, while lignin deposition in the roots is almost completely abolished in the *lac11 lac4 lac17* triple mutant [19–23]. For other species, *Miscanthus* MsLAC1 and *Pyrus bretschneideri* PbrLAC1, PbrLAC2 and PbrLAC18, as well as *Populus tomentosa* PtoLAC14 and *Cleome hassleriana* ChLAC8, were all reported to be significantly involved in lignin polymerization in various tissue types [24–27].

Laccases associated with lignin biosynthesis have been a prominent research focus in recent years for their significant disease resistance function. Among the 84 laccase genes in cotton (*Gossypium hirsutum*), GhLAC1, GhLAC4 and GhLAC15 are all implicated in disease resistance to verticillium wilt caused by *Verticillium dahliae* by enhancing G-lignin biosynthesis and lignification in the cell wall [28–31]. Laccase-induced lignification is suggested to be one of the major processes associated with the defense response in apple plant diseases, in which both *MhLAC7* and *MdLAC7* have an important function [32–34]. Tobacco overexpressing *EuLAC1* from *Eucommia ulmoides* Oliver. displayed significantly higher laccase activity and resistance to gray mold compared with wild-type tobacco [35]. However, the implication of laccase genes in grapevine lignin associated with disease resistance is little understood. Here, we characterized the laccase gene family in grapevine through bio-information analysis and analyzed the potential roles of these genes in the defense response based on the expression profile of grape leaves under infection by *B. cinerea*. The results highlight four important candidate genes, *VaLAC14*, *VaLAC19*, *VaLAC24* and *VaLAC30*, associated with lignin biosynthesis in the response against *B. cinerea*. Our work would strengthen the understanding of grape laccase genes and provide an important basis for further studying their implication in disease resistance mechanisms.

2. Materials and Methods

2.1. Plant and Fungus Materials

The leaves of Chinese wild grape (*V. amurensis* Rupr.) 'Shuangyou' (SY), a germplasm highly resistant to *B. cinerea* [36], were used as experimental plant materials. They were planted in a plant incubator at 23 °C and 75% HR (relative humidity) under a cycle of 16 h light/8 h darkness. The *B. cinerea* fungus was isolated and purified from infected grape berries. Conidia suspension, inoculation and detached leaf assay were all performed according to the description by Wan et al. [36]. The experiment was repeated three times,

and 8–10 leaves were collected repeatedly in each experiment. All treated and control (inoculated with sterile water) leaves were collected at 4, 8, 18, 36 and 72 h post-inoculation (hpi). All collected samples were immediately frozen in liquid nitrogen and stored at −80 °C for further use.

2.2. Identification of the VvLAC Gene Family

The sequence distributions of *V. vinifera* L. and *Arabidopsis thaliana* were downloaded from Ensembl Plants (http://plants.ensembl.org/index.html, accessed on 18 November 2023) and the TAIR database (http://www.arabidopsis.org/, accessed on 18 November 2023). Then, according to the conserved domain protein sequences retrieved from the Pfam database (http://pfam.sanger.ac.uk/, accessed on 18 November 2023), HMMER and BLASTP tools were used to screen the grape candidate LAC genes. The NCBI CDD database (Conserved Domain Database; http://www.ncbi.nlm.nih.gov//Structure/bwrpsb/bwrpsb.cgi, accessed on 18 November 2023) was used to analyze and identify the conserved domains of candidate *VvLAC* genes. The chromosome location information of the identified *VvLAC* genes was mapped by genome annotation files, and all the identified *VvLAC* genes were named according to the chromosome (Chr) locations. For further exploring the protein characteristics, the ExPASy protein online tool (https://web.expasy.org/compute_pi/, accessed on 22 November 2023) was used to predict the isoelectric point (pI) and molecular weight (MW) of the VvLAC proteins. WoLF PSORT (https://www.genscript.com/wolf-psort.html, accessed on 22 November 2023) was used to predict the subcellular localizations of VvLACs.

2.3. Chromosomal Location, Phylogenetic Analysis and Collinearity Analysis

MEGA software (version 10.0; Mega Limited, Auckland, New Zealand) was used to construct a phylogenetic tree with the maximum likelihood (ML) method, and the bootstrap test was repeated 1000 times [37]. Finally, the tree was annotated and decorated by ITOL online tools (http://itol.embl.de/, accessed on 10 December 2023) [38]. The phylogenetic tree was constructed based on the full-length protein sequences of LACs in *Arabidopsis thaliana* [39], *Populus trichocarpa* [40], *Citrus reticulata* Blanco [41] and *V. vinifera*. TBtools software (SCAU; version 1.0687) was used to visualize the position of grape chromosomes. The Multiple Collinearity Scan tool kit with default parameters in TBtools (version 1.0687; SCAU, Guangzhou, Guangdong, China) was used to analyze the collinearity between grape and the following herbaceous plants: *Glycine max*, *Oryza sativa* Japonica, *Gossypium raimondii* and *Arabidopsis thaliana*, and ligneous plants, *Populus trichocarpa*, *Malus domestica* Golden and *Prunus persica*.

2.4. Gene Structures, Conserved Motifs and Cis-Elements

The exon–intron structures of the *VvLAC* genes were visualized by using TBtools software (version 1.0687; SCAU, Guangzhou, Guangdong, China) by referring to the downloaded genomic information. The Multiple Em for Motif Elicitation (MEME; https://meme-suite.org/meme/tools/meme, accessed on 13 December 2023) online tool was used to analyze the conserved motifs in the *VvLAC* genes. The NCBI CDD database (Conserved Domain Database; https://www.ncbi.nlm.nih.gov/Structure/bwrpsb/bwrpsb.cgi, accessed on 13 December 2023) was used to analyze and identify the conserved domains of VvLACs. To analyze the cis-acting elements of *VvLACs*, we intercepted a sequence of 2000 bp upstream of the start codon of each *VvLAC* and then used the PlantCARE (https://bioinformatics.psb.ugent.be/webtools/plantcare/html/, accessed on 20 December 2023) online tool [42] to predict and analyze it; finally, we visualized it with TBtools (version 1.0687; SCAU, Guangzhou, Guangdong, China).

2.5. Protein Interaction Network Analysis

The homologous proteins of the AtLAC genes in *Arabidopsis thaliana* were obtained by the STRING online tool (http://string-db.org, accessed on 22 January 2024), and protein

interaction network (PPI) prediction analysis was carried out. The results were visualized by Cytoscape software (version 3.10.1; USA).

2.6. Expression Profile of Grape LAC Genes in SY Leaves against B. cinerea

RNA-seq data about the response of *VaLACs* in SY leaves against *B. cinerea* were derived from our previously published study [36].

2.7. RNA Extraction and qRT-PCR Analysis

The quantitative primers of the candidate genes were designed by Primer Premier 5.0 software (PREMIER Biosoft, San Francisco, CA, USA). The specificity of the primers was determined through NCBI (Table S1), and they were synthesized by Bioengineering Co., Ltd. (Shanghai, China). The RNA extraction kit E.Z.N.A.® Plant RNA Kit # R6827-0 (Omega Biotek, Dallas, TX, USA) was used to extract total RNA from SY leaves in the indicated infection stages. The NanoDrop 2000 instrument (Thermo Fisher Scientific, Shanghai, China) was used to check the purity and concentration of RNA, and 1% agarose gel electrophoresis was used to determine its quality. Then, according to the reverse transcription kit HiScript III qRT Super Mix for q PCR (+gDNA wiper) (Vazyme Biotech Co., Ltd., Nanjing, Jiangsu, China), the cDNAs of the corresponding samples were obtained by reverse transcription. Finally, the fluorescence quantitative PCR reaction system was configured according to the fluorescence quantitative kit ChamQ Universal SYBR qPCR Master Mix (Vazyme Biotech Co., Ltd., Nanjing, China), and qRT-PCR was performed on the CFX96 real-time system (Bio-Rad, Hercules, CA, USA). The reaction procedure was performed at 95 °C for 5 min, followed by 40 cycles at 95 °C for 15 s, 60 °C for 1 min and 72 °C for 5 min. The relative expression level of each gene was calculated by using the $2^{-\Delta\Delta t}$ method.

2.8. Determination of Laccase Activity and Lignin Content

Each leaf sample collected at the indicated time points was dried at 80 °C to constant weight, ground to powder, and sieved with a 0.425 mm aperture sieve. Then, 2 mg samples were evaluated in terms of lignin content (expressed as mg g^{-1}) by using the MZS-1-G Kit (Suzhou Comin Biotechnology Co. Ltd., Suzhou, Jiangsu, China) [43]. Then, homogenates made with 0.1 g samples with 1 mL of extracting solution in an ice bath were centrifuged at 1200 g at 4 °C for 30 min to obtain supernatant liquid. Afterwards, 45 µL of supernatant liquid was used to determine the laccase activity of each sample (expressed as nmol min^{-1} g^{-1}) by using the QM-1-G Kit (Suzhou Comin Biotechnology Co., Ltd., Suzhou, Jiangsu, China). The determination was repeated three times, and the results were expressed as means ± SEs.

2.9. Data Analysis

The data were analyzed by using SPSS version 20 (IBM SPSS Inc., Chicago, IL, USA). Statistical significance was analyzed by Duncan's test. Different lowercase letters indicated that the difference among treatments reached a significant level ($p \leq 0.05$).

3. Results

3.1. Laccase Activity and Lignin Content in SY Leaves in Response to B. cinerea

The phenotypic characteristics of grape leaves inoculated with *B. cinerea* conidia 4–72 hpi verified that SY was resistant against the pathogen (Figure 1a). In control samples, laccase activity and lignin biosynthesis almost showed no significant change. After infection, laccase activity showed a significant increase 18 hpi and was significant higher in the infected SY leaves than in the control samples from 8 hpi onwards. Lignin content in the *B. cinerea*-infected SY leaves was increased 4 hpi and was also significantly higher than in the control samples from then on, except at 36 hpi (Figure 1b,c).

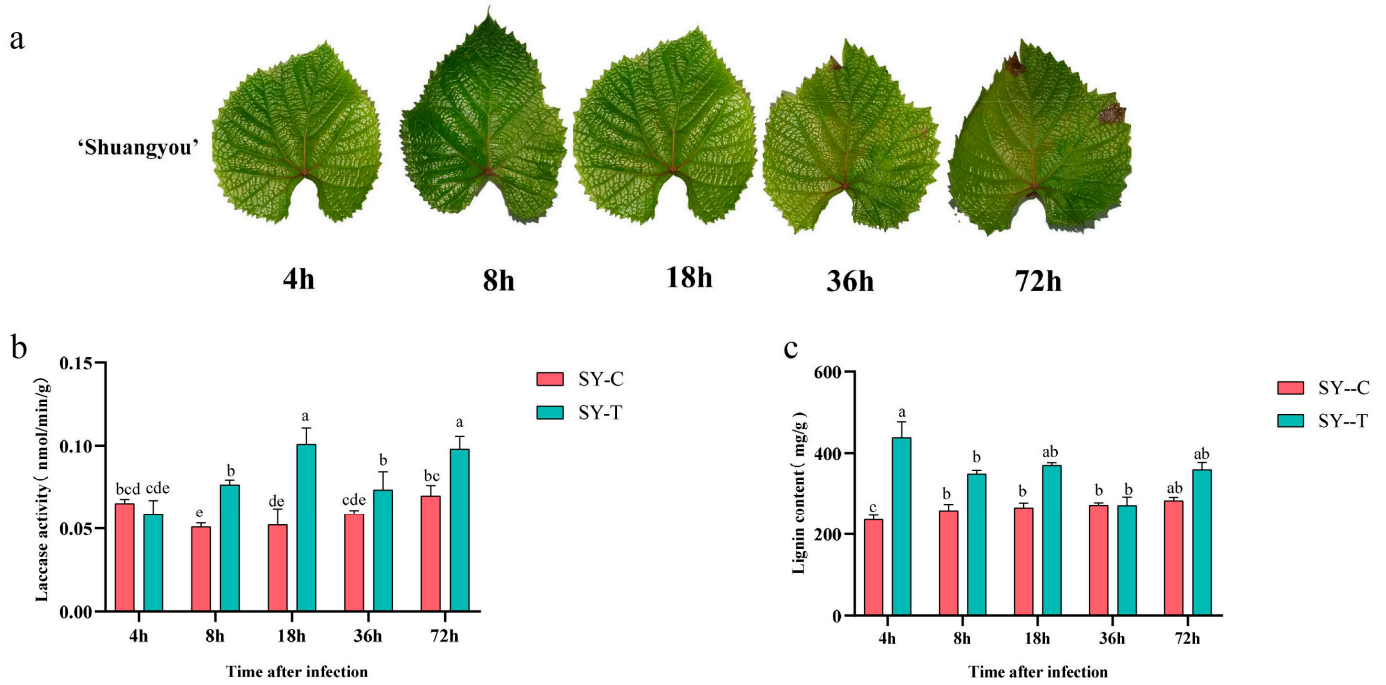

Figure 1. Changes in resistant 'Shuangyou' grape leaves. (**a**) Phenotypic observation. (**b**) Laccase activity and (**c**) lignin content. C: control (inoculation with sterile water); T: treatment (inoculation with *Botrytis cinerea*). SY: Chinese wild *V. amurensis* 'Shuangyou', a germplasm highly resistant to *B. cinerea*. The results are the means (SDs) of three biological replicates. There were significant differences between the results marked with different lowercase letters ($p \leq 0.05$).

3.2. Identification of VvLAC Genes in Grapevine

A total of 30 members of the *VvLAC* gene family were retrieved from the 'Pinot Noir' *Vitis* genome (PN40024.v4) and were renamed from *VvLAC1* to *VvLAC30* according to their positions on the Chrs (Table 1). The length of their encoding proteins ranged from 386 to 627 amino acids, and the molecular weights of the proteins ranged from 42.46 to 69.76 KDa (Table 1). The theoretical isoelectric points of these proteins ranged from 4.79 to 9.79, with VvLAC28 showing the lowest value and VvLAC11 the highest one; they comprised 24 basic proteins and 6 acidic proteins distributed on Chr 18, except for VvLAC14, which was found on Chr 8 (Table 1). Moreover, the subcellular localization displayed that 17 VvLAC proteins were located on chloroplasts, followed by the vacuolar membrane and extracellular matrix, each with 4 VvLAC proteins; the cytoskeleton, with 3 proteins; and the plasma membrane and peroxisome, with the lowest number of protein, with 1 VvLAC protein each.

Table 1. Information of the *VvLAC* gene family.

Name	Gene ID	Chromosome	Gene Length (bp)	pI	MW (Kda)	Amino Acid (aa)	Subcellular Localization
VvLAC1	Vitvi04g01317_t001	Chr4	1692	8.49	62.23	563	vacu
VvLAC2	Vitvi06g00378_t001	Chr6	1758	9.02	64.39	585	chlo
VvLAC3	Vitvi06g00405_t001	Chr6	1758	8.71	64.30	585	extr
VvLAC4	Vitvi06g00591_t001	Chr6	1665	9.26	60.70	554	chlo
VvLAC5	Vitvi06g00728_t001	Chr6	1725	8.59	63.59	574	vacu
VvLAC6	Vitvi08g01031_t001	Chr8	1689	8.37	62.49	562	extr
VvLAC7	Vitvi08g01223_t002	Chr8	1641	9.32	59.90	546	chlo
VvLAC8	Vitvi08g01223_t001	Chr8	1740	9.24	63.69	579	chlo
VvLAC9	Vitvi08g04233_t001	Chr8	1197	9.74	43.53	398	chlo
VvLAC10	Vitvi08g02201_t001	Chr8	1734	9.77	64.04	577	chlo
VvLAC11	Vitvi08g01228_t001	Chr8	1734	9.79	64.04	577	chlo

Table 1. *Cont.*

Name	Gene ID	Chromosome	Gene Length (bp)	pI	MW (Kda)	Amino Acid (aa)	Subcellular Localization
VvLAC12	Vitvi08g04234_t001	Chr8	1734	9.78	64.08	577	chlo
VvLAC13	Vitvi08g01229_t001	Chr8	1761	9.22	64.96	586	chlo
VvLAC14	Vitvi08g01299_t001	Chr8	1698	6.79	62.00	565	vacu
VvLAC15	Vitvi08g01335_t001	Chr8	1671	9.12	60.48	556	chlo
VvLAC16	Vitvi08g01735_t001	Chr8	1674	8.04	61.69	557	extr
VvLAC17	Vitvi13g00117_t001	Chr13	1734	7.63	63.18	577	cyto
VvLAC18	Vitvi13g00321_t001	Chr13	1752	9.44	64.30	583	chlo
VvLAC19	Vitvi13g00322_t001	Chr13	1752	9.53	64.39	583	chlo
VvLAC20	Vitvi13g00323_t001	Chr13	1755	9.35	64.61	584	vacu
VvLAC21	Vitvi13g00341_t001	Chr13	1755	9.4	64.50	584	chlo
VvLAC22	Vitvi13g00342_t001	Chr13	1755	9.22	64.45	584	chlo
VvLAC23	Vitvi13g00509_t001	Chr13	1662	8.67	60.40	553	chlo
VvLAC24	Vitvi15g00941_t001	Chr15	1884	8.19	69.76	627	chlo
VvLAC25	Vitvi17g00227_t001	Chr17	1752	8.5	65.26	583	chlo
VvLAC26	Vitvi18g01488_t001	Chr18	1776	5.3	66.34	591	extr
VvLAC27	Vitvi18g02924_t001	Chr18	1791	4.89	66.31	596	cyto
VvLAC28	Vitvi18g02922_t001	Chr18	1794	4.79	66.25	597	pero
VvLAC29	Vitvi18g02927_t001	Chr18	1779	5.52	66.58	592	plas
VvLAC30	Vitvi18g02928_t001	Chr18	1800	4.92	67.64	599	cyto

Note: vacu: vacuolar membrane; chlo: chloroplast; extr: eextracellular matrix; cyto: cytoskeleton; pero: peroxisome; plas: plasma membrance.

3.3. Chromosomal Locations and Phylogenetic Analysis

In the present study, 30 *VvLAC* genes were distributed on seven different chromosomes (Figure 2a). It was found that 11 of them were mainly located on Chr 8 (*VvLAC6–16*), 7 on Chr 13 (*VvLAC17–23*), 5 on Chr 18 (*VvLAC26–30*) and 4 on Chr 6 (*VvLAC2–5*), together containing 27 *VvLAC* genes, while Chr 4, Chr 15 and Chr 17 only contained 1 *VvLAC* gene each. The results show no positive correlation between chromosome length and number of *VvLAC* genes. Moreover, some members of the *VvLAC* family on Chr 8, Chr 13 and Chr 18 exist in the form of gene clusters.

To explore the evolutionary relationships of *VvLACs*, a phylogenetic analysis was performed based on the full-length amino acid sequences of 30 VvLACs and the LAC proteins from other plant species, which included 17 LACs from *Arabidopsis thaliana*, 53 from *Populus trichocarpa* and 27 from *Citrus reticulata*. According to the classification standard of *Arabidopsis thaliana* laccases, 30 VvLACs and 97 LACs were divided into seven groups, and their distribution in each group was rather uneven (Figure 2b). In detail, only 1 VvLAC was clustered with 2, 6 and 12 LACs in Group I, Group II and Group III, respectively. Also, Group IV contained 2 VvLACs, VvLAC5 and VvLAC17, together with 15 LACs (Figure 2b). Moreover, 22 and 29 LACs were classified in Group V and Group VI, each with 5 VvLAC, whereas Group VII contained the maximum number of LAC proteins, up to 37 LACs, in which there were 15 VvLACs (Figure 2b). In addition, it was found that all the 5 VvLACs clustered in Group V were located on Chr 18, while 8 out of the 11 VvLACs on Chr 13 all belonged to Group VII (Figure 2). These results indicate that specific evolutionary events occurred among *VvLAC* genes after the divergence of grapevine and the other three plants.

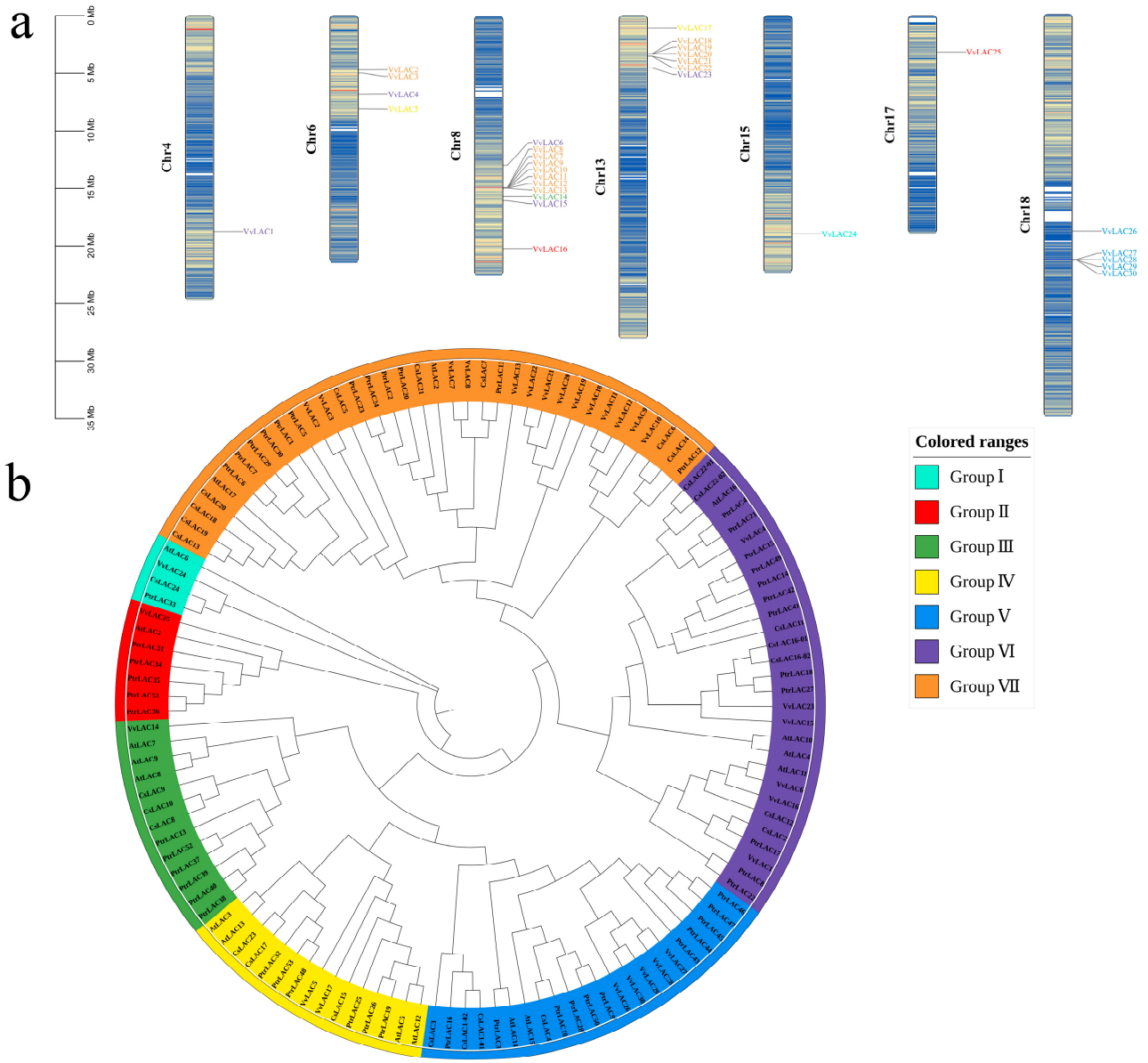

Figure 2. Chromosomal localization and phylogenetic analysis. (**a**) The chromosomal localization of the *VvLAC* gene family. Genes in the same subgroup are represented by the same color. The left ruler indicates the length of the grape chromosomes. (**b**) The phylogenetic tree was constructed based on the protein sequences from *Arabidopsis thaliana*, *Populus trichocarpa* and *Citrus reticulata* Blanco. The adjacency tree was constructed by using MEGA10.0. The seven groups are distinguished by different colors.

3.4. Gene Duplication and Syntenic Analysis

Generally, gene duplication, including tandem repeats, and segmental and tandem duplication, is one of the most important driving forces leading gene expansion and evolution during genome evolution [44,45]. It plays important roles in improving plant adaptability to various environmental stresses [45]. To understand the gene duplication pattern of *VvLACs*, a collinearity analysis was performed in this study. As a result, 11 *VvLAC* duplicated geneswere distributed on seven chromosomes (including Chr 6, Chr 13 and Chr 8), among which *VvlAC18–20* were found to be tandem repeat genes, and so were *VvlAC9*, *VvLAC11* and *VvLAC13* (Figure 3a).

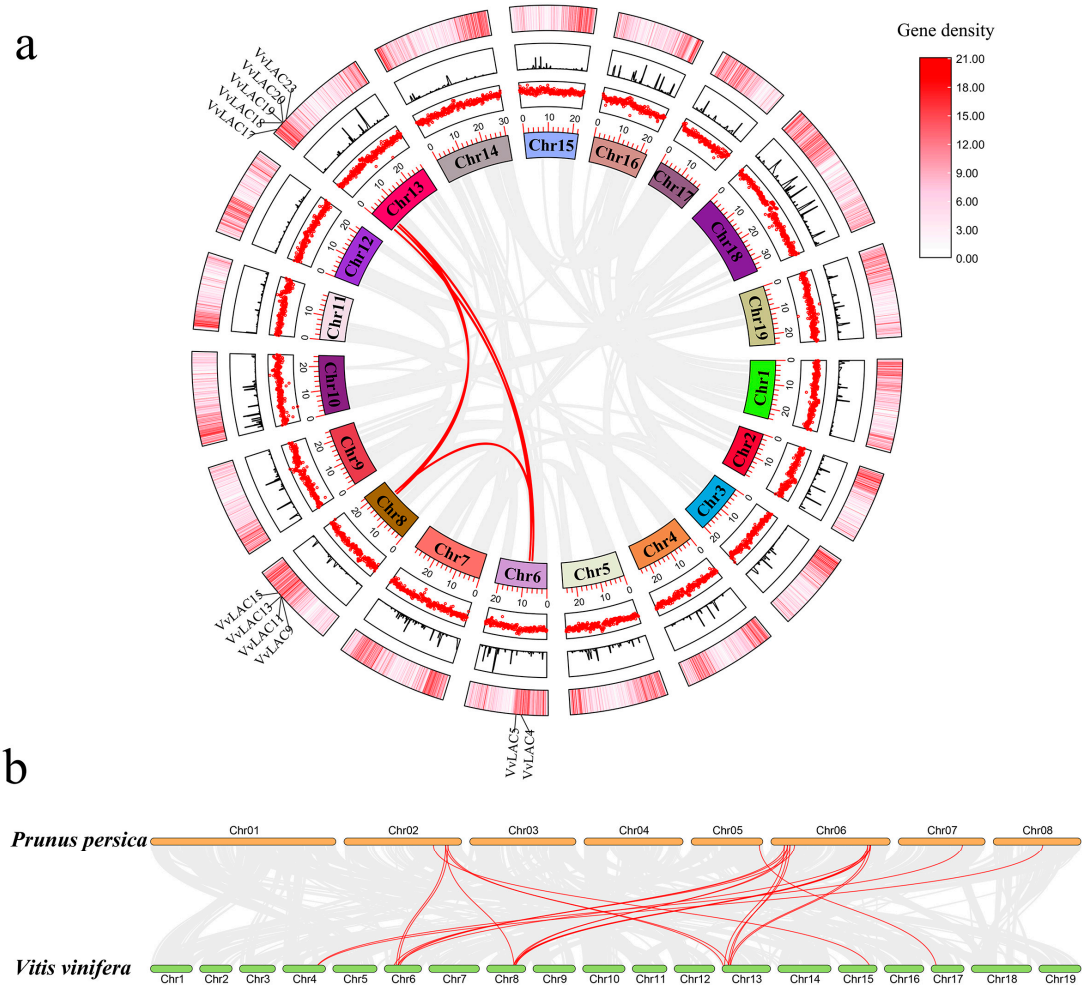

Figure 3. Interspecific and intraspecific collinearity analyses of the *VvLAC* genes. (**a**) Intraspecific collinearity analysis. The innermost circle shows the 19 chromosomes of *Vitis vinifera*. Different chromosomes are represented by different colors, followed by N ratio and G/C ratio. The outermost circle shows the gene densities on the corresponding chromosomers, and a redder color represents a higher gene densities. The identified *VvLAC* gene pairs are linked by red lines. (**b**) Syntenic analysis of *Prunus persica* and *Vitis vinifera LAC* genes. The different chromosomes of the two are represented by different colors. The gray lines represent the collinear lines in the genome of the two plants, while the red lines highlight the same line of the LAC gene pair.

Furthermore, a syntenic analysis was performed for predicting the function of *VvLACs* through the homology analysis of *LAC* genes from four herbaceous plants and three ligneous plants. In total, 22 syntenic gene pairs between grape and *Prunus persica* were observed; however, no syntenic gene pairs were present (Figure 3b), which may relate to the weaker phylogenetic relationships between grape and the other six plant species.

3.5. Motif Composition and Gene Structure

A total of 10 types of conserved motifs of the VvLAC family genes were explored by using the MEME program (Figure 4). Many classes of VvLAC proteins were found to have quite consistent motif compositions, except for VvLAC9, which was composed of only six motifs (Figure 4a). This suggests that functional redundancy possibly exist among these genes. Also, motif variations in numbers, amino acids and lengths across VvLACs were observed (Figure 4b), and as a result, their functional divergence was hypothesized. As expected, all the identified VvLAC proteins contained the conserved functional laccase domain (Figure 4c).

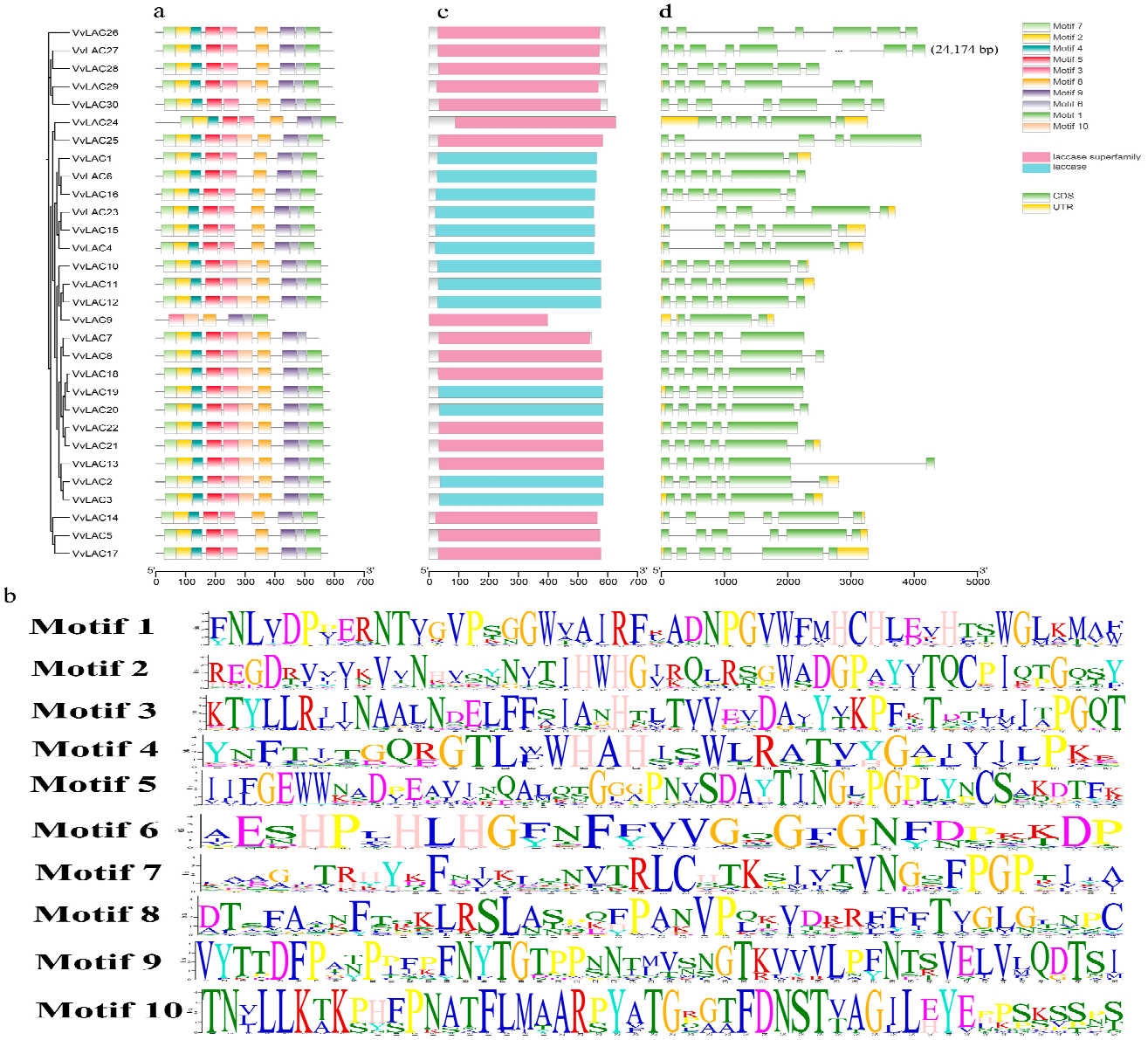

Figure 4. Motif composition and gene structure analyses of *VvLACs*. (**a**,**b**) Motif information. (**c**) Conserved domain. (**d**) Intron–exon patterns. UTR and CDS are represented by yellow boxes and green boxes, respectively.

To further investigate gene evolution, the exon–intron distribution of *VvLACs* was analyzed by aligning coding sequences against their corresponding genomic sequences. The results show that the gene structures of *VvLACs* exhibit diverse intron–exon patterns (Figure 4d). For example, except for *VvLAC9*, which has only four exons, the exon number varies from five to seven among the *VvLAC* genes. Notably, there are five genes, all in Group V, containing the highest number of exons, seven, with *VvLAC27* being the longest gene, with 24,174 bp in total. Generally, *VvLACs* displaying high homology have highly similar gene structures (Figure 4).

Subsequently, the amino acid sequences of all the AtLACs and VvLACs were aligned together. The results show that the VvLAC proteins have higher similarity with the AtLAC proteins and have three canonical plant laccase Cu oxidase domains, namely, Cu RO_1_LCC_plant, Cu RO_2_LCC_plant and Cu RO_3_LCC_plant (Figure 5).

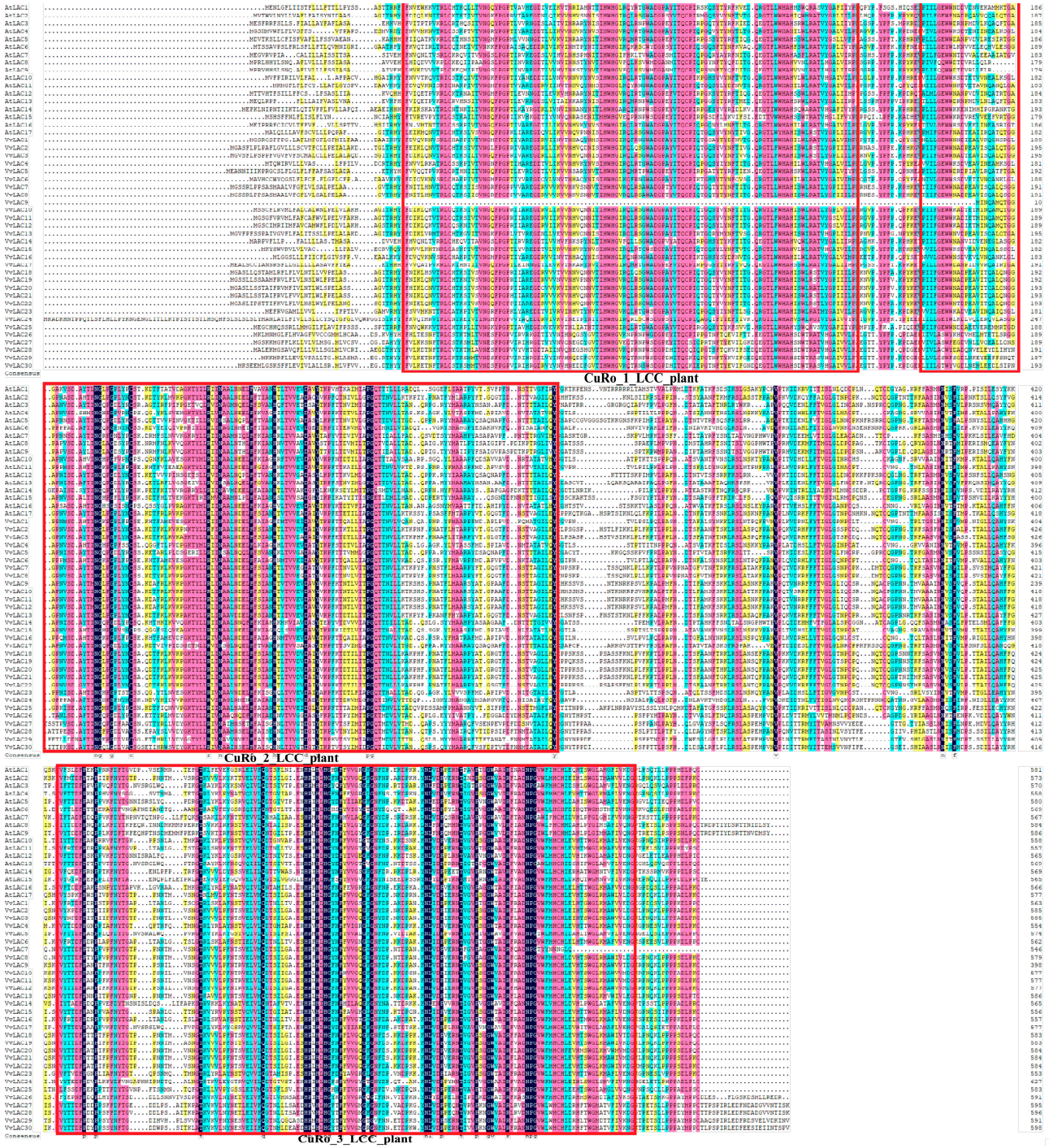

Figure 5. VvLACs and AtLAC protein sequence alignment analysis.

3.6. Cis-Elements in Promoters of VvLAC Genes

To explain their transcriptional differences, we analyzed the cis-elements in the promoter regions of the laccase gene family. Sixty–eight *cis*-elements were observed in *VvLAC* promoters and classified into the seven categories shown in Figure 6. The light-responsive elements, phytohormone elements, biotic/abiotic stress elements and MYB-TF (transcriptional factor) elements were the most frequently identified in the promoter regions of the grape laccase genes. Among all the elements, the MYB elements were the most prominent, and the only ones present in each *VvLAC* promoter, reaching the maximum of 11 in *VvLAC6*, *VvLAC16* and *VvLAC19* (Figure 6). Meanwhile, the MYC element was specially noticed, being present the most among phytohormone elements, except in the promot-

ers of *VvLAC29* and *VvLAC30*. Also, STRE (stress response promoter element), W-box (WRKY-binding site [36]) and WRE3 were relatively abundant among biotic/abiotic stress elements (Figure 6). Moreover, there were 22 types of light-responsive elements, and Box 4, GT1-motif, G-box and GATA-motif were abundantly detected (Figure 6).

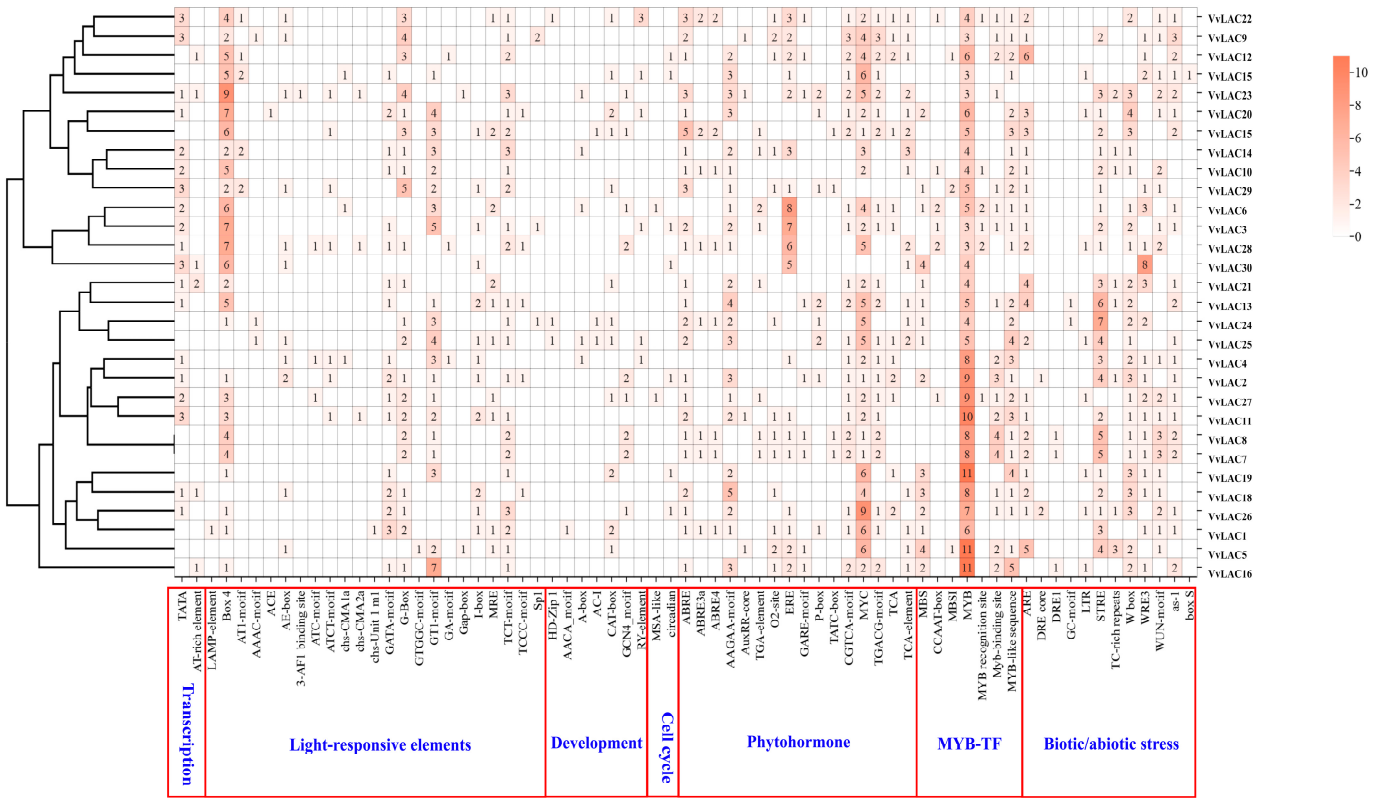

Figure 6. Identification of *cis*-elements in the upstream promoters of the indicated *VvLAC* genes. The heat map was generated based on the numbers and predicted functions of the *cis*-elements. Different colors and numbers in the grid represent the number of the corresponding *cis*-elements in each *VvLAC* gene promoter.

3.7. Protein–Protein Interaction Network

To investigate whether the VvLAC proteins might function by forming homo- or hetero-protein complexes, we constructed a protein interaction network for VvLACs based on their orthology with AtLAC proteins (Figure 7, Table S2). A total of 62 interacting protein pairs composed of 30 VvLACs and 11 VtLACs were predicted and divided into 11 subfamilies. There were no direct interactions between the VvLACs themselves, and the interacting proteins mainly included six types, PAL1-4 and CCR1/2, except for the 11th subfamily, which had distinct types, including PAL1/4, CESA4/7/8 and MYB63, T25K17.30, CESA4/7/8, PAL1, PAL1/2/4 and CCR1/2 were all predicted to interact with the VvLAC2, VvLAC7/8 and VvLAC1/6/16 proteins in the first, second and eighth subfamilies, respectively (Figure 7, Table S2). The fifth, sixth and seventh subfamilies, including VvLAC24, VvLAC14 and VvLAC15, respectively, revealed the same interaction proteins, PAL1-4 and CCR1. Additionally, both the third (VvLAC17) and tenth (VvLAC4 and VvLAC23) subfamilies contained T25K17.30 and PAL1-4. Additionally, PAL1-3 and CCR1/2 were predicted as the interaction proteins of VvLAC29-30 in the ninth subfamily, while VvLAC17 in the fourth subfamily was linked with the T25K17.30, PAL1/2 and CCR1/2 interaction proteins (Figure 7, Table S2).

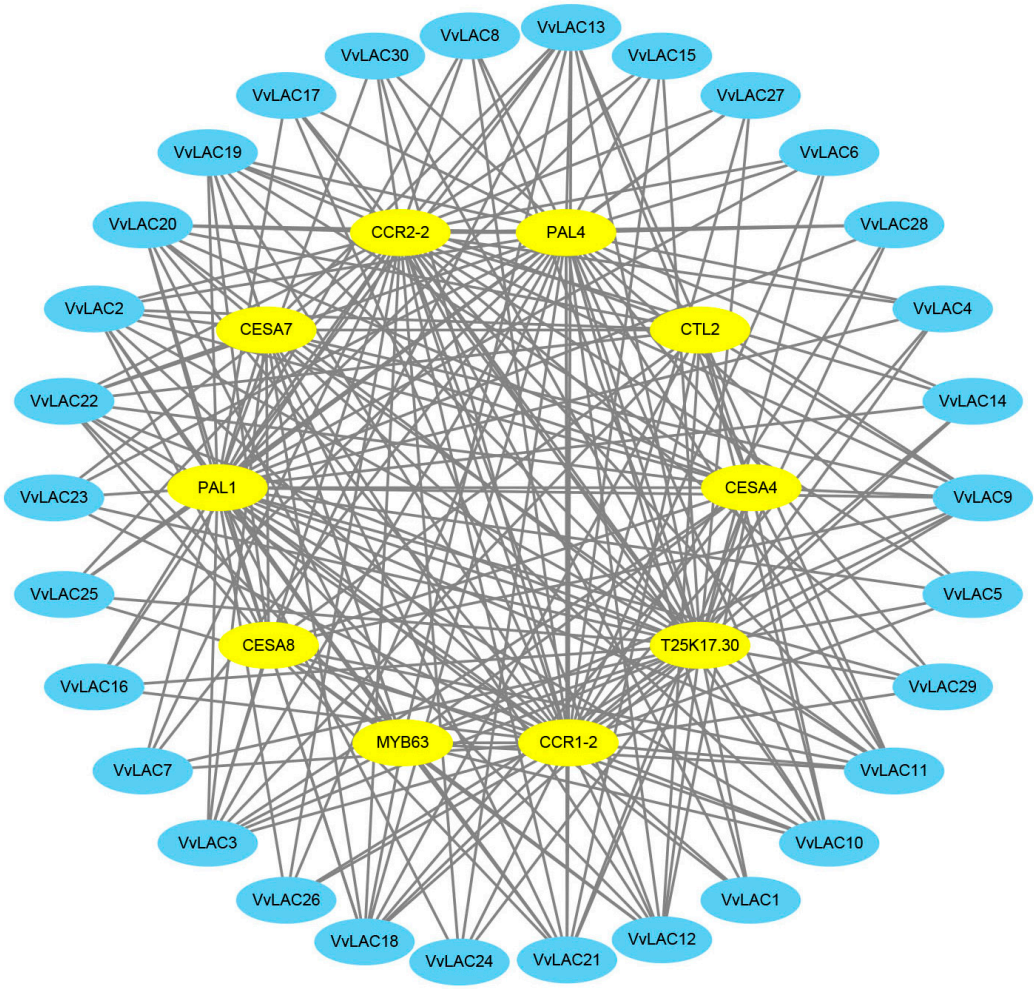

Figure 7. Prediction of protein–protein interaction network of VvLACs based on AtLACs in *Arabidopsis thaliana*. VvLAC proteins are shown in blue circles and the predicted interaction proteins are shown in yellow circles.

3.8. Expression Profiles of LAC Genes in SY Leaves in Response against Botrytis cinerea

The expression patterns of all the 30 *LAC* genes were analyzed based on the RNA-seq data of the SY leaves in the early interaction stages, 4–36 after inoculation with *B. cinerea* and sterile water [36]. There were four genes previously annotated as *LACs* according to the RNA-seq data; however, in the present study, each was actually identified to be containing two *LACs* according to the latest released grape genomic annotation version (PN40024. v4). These grape genes are *LAC7/8*, *LAC11/12*, *LAC19/20* and *LAC21/22*. Even so, we obviously found several genes with different expression in the infected SY leaves compared with the control leaves, for example, *VaLAC14*, *VaLAC24*, *VaLAC30*, *VaLAC17* and so on (Figure 8a). Relative quantification was used to confirm the expression levels of the selected genes as shown in Figure 8b. The results show that in contrast with other *VaLAC* genes, the similar trends of expression of *VaLAC14* and *VaLAC24* were significantly high in the SY leaves during infection by *B. cinerea* (Figure 8b). After *B. cinerea* infection, the expression levels of *VaLAC13*, *VaLAC30* and *VaLAC25* significantly increased, especially from 4 hpi to 8 hpi and following 36 hpi. Also, *VaLAC19* expression was significantly increased from 4 hpi to 18 hpi (Figure 8b). Despite displaying significant changes, the relative expression of the remaining *VaLAC* genes following infection was very low (Figure 8b).

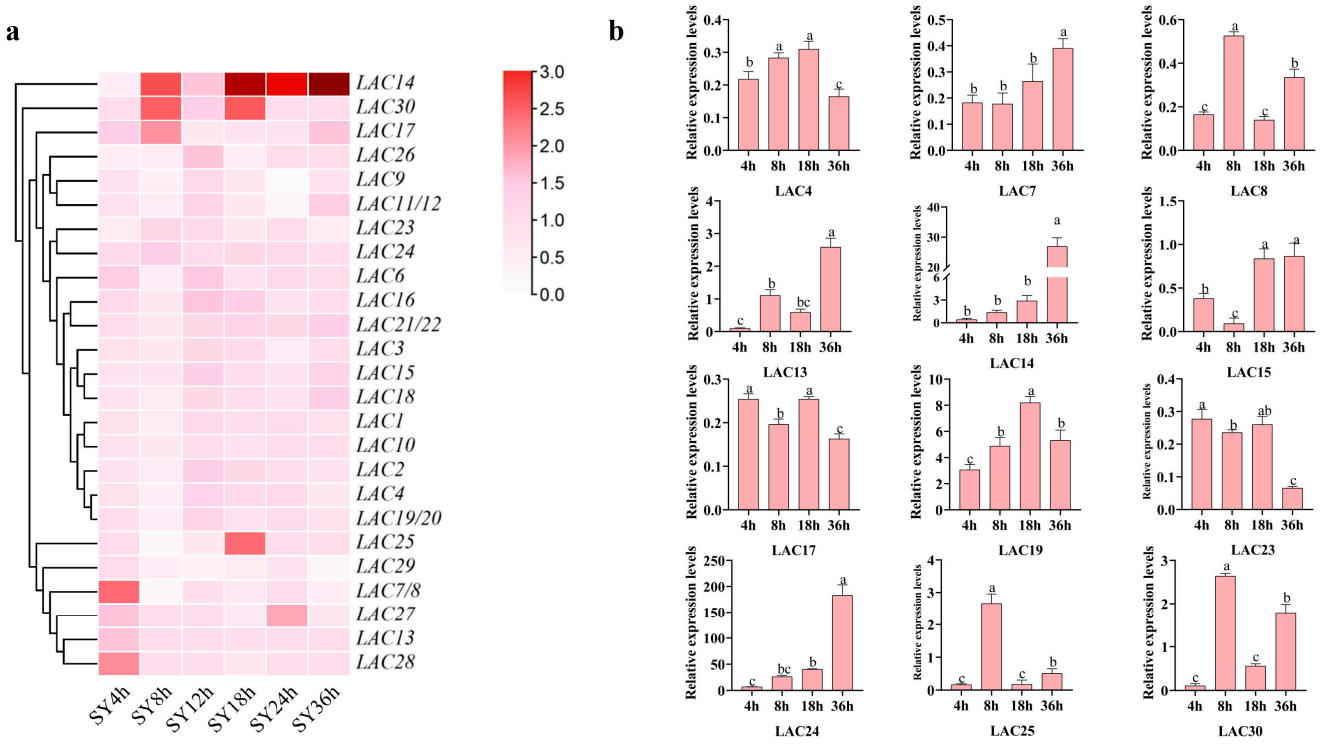

Figure 8. The expression analysis of the *VaLACs* in the SY response to *B. cinerea*. (**a**) The ratios of *VaLAC* expression after infection compared with the control, which were derived from previously published RNA-Seq data on the interaction between SY leaves and *B. cinerea* at the indicated time points after infection [36]. (**b**) The relative expression levels of the selected *VaLAC* genes determined through qRT-PCR. SY: Chinese wild *V. amurensis* 'Shuangyou', a germplasm highly resistant to *B. cinerea*. The expression value was reported as the mean ± standard deviation of three independent biological replicates, where each biological replicate contained three technical replicates. Different letters in the figure indicate significant differences, $p < 0.05$. C: control (inoculation with sterile water); T: treatment (inoculation with *B. cinerea*).

4. Discussion

Laccase is a multi-copper oxidase that catalyzes the oxidation of a wide range of phenolic compounds and has been widely and traditionally researched for potential applications in the food, pharmaceutical and environmental industries for its eco-friendly catalysis [46]. In recent decades, increasing numerous studies have demonstrated that plant LACs, a family of key enzymes polymerizing lignin monomers into lignins, play multiple roles in development and response to biotic and abiotic stresses [19,28,33,34,44]. Systematic analyses have been conducted to identify laccase gene families in many model plants, as well as crop, woody and horticultural plants. The laccase gene families in *Arabidopsis thaliana* (17) [47], *Oryza sativa* (30) [48], *Populus trichocarpa* (49) [40], *Brassica rapa* var. pekinensis (27) [49], *Brassica rapa* var. rapa (27) [49], *Bretschneideri* (45) [25], *Citrus sinensis* (41) [41] and *Punica granatum* (57) [43] have been revealed. Comparatively, *Triticum aestivum* (95) [50], soybean (93) and *Gossypium hirsutum* (84) [28] have more *LAC* members.

Grape is one of the most important horticultural crops in the world. We found that the *B. cinerea*-resistant grape germplasm SY significantly increased the lignin levels in accordance with the increase in laccase activity after infection. Considering the crucial roles of lignin in plant disease resistance [9,11], it might be an important characteristic for SY resistance to *B. cinerea*. Thus far, the laccase gene family members have been little studied in grapevine. Here, a total of 30 *VvLACs* were identified based on the grapevine genome in public databases, and a comprehensive analysis of the *VvLAC* gene family was performed. In grapevine, 30 *VvLACs* are unevenly distributed on seven chromosomes, including 6 tandem repeat genes and 5 segmentally duplicated genes on three chromosomes. Gene

duplication events, including tandem repeat and segmental duplication, contributed to grape LAC gene family expansion and evolution. Moreover, syntenic pairs were only observed between grape and peach *LAC* genes, and they might have little evolution relationship with the other six species, including *Arabidopsis thaliana* and *Malus domestica*, in the present study. Motif and gene structure analyses showed that the closely related grape *LAC* members in the phylogenetic tree had similar exon–intron structures and common motif compositions, indicating a possible functional similarity. Diversities in gene structures and motif composition across different groups were also found, indicating functional differentiation in grape laccases.

Here, 30 VvLACs were classified into seven groups according to the classification criteria applied in *Arabidopsis thaliana* [39,47]. AtLAC15 in Group V, AtLAC4 and AtLAC11 in Group VI, and AtLAC2 and AtLAC17 in Group VII have been demonstrated to have a defined function in lignin biosynthesis [19–23]. PbrLAC1 and PbrLAC2 homologous with AtLAC4 and PbrLAC18 homologous with AtLAC17 have been proved to regulate lignin biosynthesis in pear stone cells [25]. This implies that as many as 25 VvLACs in the three groups are probably implicated in grape lignin biosynthesis. Combined for their quite consistent motif compositions and structures, these grape *LAC* genes possibly present functional redundancy. Recent research results also support the point that functional redundance exist in multiple *LAC* genes from one species. In *Arabidopsis thaliana* or pear, each single-laccase-gene-mutant or -silenced strain only slightly reduced the lignin content, whereas the simultaneous mutation or silencing of at least two laccase genes led to a significant decrease in lignin content [23,26].

V. amurensis, the most cold-tolerant *Vitis* species, is suggested to be highly resistant to *B. cinerea* and to share a common ancestor with *V. vinifera* dating approximately 2 million years ago [3,45,51]. *VaERF16*, *VaMYB306* and *VaERF20* from *V. amurensis* have been revealed to have a resistant function in *B. cinerea* infection [52,53]. Here, the expression profile of *V. amurensis* SY *LAC* genes highlighted the candidates *VaLAC14*, *VaLAC24*, *VaLAC30*, *VaLAC13*, *VaLAC19* and *VaLAC25* as being significantly involved in the grape response to *B. cinerea*. In Group III, VvLAC14 was clustered with AtLAC7, AtLAC8 and AtLAC9, whose expression is induced under environmental stress [39]. *VaLAC14* and *VaLAC24*, having similar expression trends, might both play potential roles in the response of grapevine to *B. cinerea*. In Group V, VvLAC30 was clustered with AtLAC15. In cotton, GhLAC15, which is phylogenetically related to AtLAC15, was reported to positively regulate disease-induced lignification to enhance resistance to broad-spectrum biotic stress response [30]. Here, *VaLAC30* was suggested to be involved in the SY defense against the fungus through lignin enhancement. Grape LAC13 and LAC19 were both clustered with AtLAC17 and PtrLAC23 in Group VII, implying their possible roles in grape lignin biosynthesis to resist to the fungus. PtrLAC23 was confirmed to have the function of lignin deposition in *Populus trichocarpa* stem transects through transgenic experiments [40]. VaLAC25 was in Group II with AtLAC1, PtrLAC31 and PtrLAC34, which are mainly expressed in plant roots and leaves [39,40], while their implication in lignin biosynthesis and plant disease, including *VaLAC25*, in the grape response to *B. cinerea* remains to be revealed in future.

To understand the potential regulation of grape *LAC* expression, we analyzed the *cis*-elements of *VvLACs*, and seven classes of cis-elements were obtained. The putative *cis*-elements suggest that *VvLACs* participate in many physiological processes, such as development, and light and stress responses. MYB and WRKY are significant regulators in the plant defense response to *B. cinerea*, and they can interact with genes associated with cell wall metabolism [36,54]. Notably, the MYB *cis*-element was present in all *VvLAC* promoters. AtMYB58 and AtMYB63, directly interacting with *AtLAC4*, are specific transcriptional activators of lignin biosynthesis [55]. Therefore, we predicted that MYB may have crucial roles in *B. cinerea* resistance by targeting *LACs* in grape leaves, but further research is needed. The *VvLAC19* promoter had three WRKY-targeting W-box *cis*-elements, and *MdLAC7* can be bound by MdWRKY75 to improve apple resistance to *A. alternata* by increasing the biosynthesis of laccase and lignin [33]. There might be other regulators besides MYB and

WRKY in this response of grapevine. The stress *cis*-element STRE was also observed in candidate *VvLAC13*, *VvLAC24* and *VvLAC25* promoters. The STRE *cis*-element is a stress response promoter element widely involved in responding to various stressors, e.g., salt, water and heat, and is regulated by the transcriptional factors of zinc finger proteins and heat shock factors [56,57].

5. Conclusions

Laccases have been revealed to play important roles in plant disease resistance associated with lignin biosynthesis in recent years. However, information on grape laccase activity in the defense against *B. cinerea* is largely unknown. In the present study, a total of 30 grape laccase genes from the *V. vinifera* genome were identified and divided into seven groups. The proteins containing three typical plant Cu-oxidase domains displayed high conservation among each other. The phylogenetic analysis indicated that up to 25 *VvLACs* might be related to grape lignin biosynthesis, also implying a possible redundant function. The *cis*-element analysis highlighted MYB's and WRKY's regulating roles in grape *LAC* expression. Further investigation of *LAC* gene expression in *B. cinerea*-resistant Chinese wild *V. amurensis* 'Shuangyou' revealed that *VaLAC14*, *VaLAC19*, *VaLAC24* and *VaLAC30* could potentially act as the key candidate genes in lignin biosynthesis in the grape response to *B. cinerea*. This study lays the foundation for understanding the grape *LAC* genes and their roles in the response to *B. cinerea*. How these candidate genes participate in *B. cinerea* resistance by regulating lignification needs to be further verified.

Supplementary Materials: The following supporting information can be downloaded at: https://www.mdpi.com/article/10.3390/horticulturae10040376/s1, Table S1: Primers of selected *VaLAC* genes used for qRT-PCR, Table S2: Information on protein–protein network prediction.

Author Contributions: Conceptualization, R.W., Z.Y., J.S. and X.Z.; formal analysis, Z.Y., J.L., M.Z. and J.J.; visualization, R.W., Z.Y., M.W. and C.S.; investigation, Z.Y., J.L., J.S., Y.L. and K.Z.; resources, R.W., X.Z., P.H. and T.B.; writing—original draft, R.W. and Z.Y.; writing—review and editing, R.W., S.S., J.S. and X.Z. All authors have read and agreed to the published version of the manuscript.

Funding: We appreciate the support from Natural Science Foundation of Henan province (222300420182) and National Natural Science Foundation of China (32302495).

Data Availability Statement: The original contributions presented in the study are included in the article and supplementary materials.

Conflicts of Interest: The authors declare no conflicts of interest.

References

1. Shen, F.; Wu, W.; Han, X.; Wang, J.; Li, Y.; Liu, D. Study on the occurrence law and green control of grape gray mold from the perspective of ecological balance. *Bioengineered* **2021**, *12*, 779–790. [CrossRef] [PubMed]
2. De Simone, N.; Pace, B.; Grieco, F.; Chimienti, M.; Tyibilika, V.; Santoro, V.; Capozzi, V.; Colelli, G.; Spano, G.; Russo, P. *Botrytis cinerea* and table grapes: A review of the main physical, chemical, and bio-based control treatments in post-harvest. *Foods* **2020**, *9*, 1138. [CrossRef] [PubMed]
3. Wan, R.; Hou, X.; Wang, X.; Qu, J.; Singer, S.D.; Wang, Y.; Wang, X. Resistance evaluation of Chinese wild *Vitis* genotypes against *Botrytis cinerea* and different responses of resistant and susceptible hosts to the infection. *Front. Plant Sci.* **2015**, *6*, 160149. [CrossRef] [PubMed]
4. Harper, L.A.; Paton, S.; Hall, B.; McKay, S.; Oliver, R.P.; Lopez-Ruiz, F.J. Fungicide resistance characterized across seven modes of action in *Botrytis cinerea* isolated from Australian vineyards. *Pest Manag. Sci.* **2022**, *78*, 1326–1340. [CrossRef] [PubMed]
5. Bi, K.; Liang, Y.; Mengiste, T.; Sharon, A. Killing softly: A roadmap of *Botrytis cinerea* pathogenicity. *Trends Plant Sci.* **2023**, *28*, 211–222. [CrossRef]
6. Blanco-Ulate, B.; Morales-Cruz, A.; Amrine, K.C.H.; Labavitch, J.M.; Powell, A.L.T.; Cantu, D. Genome-wide transcriptional profiling of *Botrytis cinerea* genes targeting plant cell walls during infections of different hosts. *Front. Plant Sci.* **2014**, *5*, 98301. [CrossRef] [PubMed]
7. Veloso, J.; van Kan, J.A.L. Many shades of grey in *Botrytis*-host plant interactions. *Trends Plant Sci.* **2018**, *23*, 613–622. [CrossRef] [PubMed]
8. Goetz, G.; Fkyerat, A.; Métais, N.; Kunz, M.; Tabacchi, R.; Pezet, R.; Pont, V. Resistance factors to grey mould in grape berries: Identification of some phenolics inhibitors of *Botrytis cinerea* stilbene oxidase. *Phytochemistry* **1999**, *52*, 759–767. [CrossRef]

9. Liu, Q.; Luo, L.; Zheng, L. Lignins: Biosynthesis and biological functions in plants. *Int. J. Mol. Sci.* **2018**, *19*, 335. [CrossRef] [PubMed]
10. Lazniewska, J.; Macioszek, V.K.; Kononowicz, A.K. Plant-fungus interface: The role of surface structures in plant resistance and susceptibility to pathogenic fungi. *Physiol. Mol. Plant Pathol.* **2012**, *78*, 24–30. [CrossRef]
11. Lee, M.-H.; Jeon, H.S.; Kim, S.H.; Chung, J.H.; Roppolo, D.; Lee, H.-J.; Cho, H.J.; Tobimatsu, Y.; Ralph, J.; Park, O.K. Lignin-based barrier restricts pathogens to the infection site and confers resistance in plants. *Embo J.* **2019**, *38*, e101948. [CrossRef] [PubMed]
12. Asselbergh, B.; Curvers, K.; Franca, S.C.; Audenaert, K.; Vuylsteke, M.; Van Breusegem, F.; Hoefte, M. Resistance to *Botrytis cinerea* in sitiens, an abscisic acid-deficient tomato mutant, involves timely production of hydrogen peroxide and cell wall modifications in the epidermis. *Plant Physiol.* **2007**, *144*, 1863–1877. [CrossRef] [PubMed]
13. Lloyd, A.J.; Allwood, J.W.; Winder, C.L.; Dunn, W.B.; Heald, J.K.; Cristescu, S.M.; Sivakumaran, A.; Harren, F.J.M.; Mulema, J.; Denby, K.; et al. Metabolomic approaches reveal that cell wall modifications play a major role in ethylene-mediated resistance against *Botrytis cinerea*. *Plant J.* **2011**, *67*, 852–868. [CrossRef] [PubMed]
14. Xue, M.; Yi, H. Induction of disease resistance providing new insight into sulfur dioxide preservation in *Vitis vinifera* L. *Sci. Hortic.* **2017**, *225*, 567–573. [CrossRef]
15. Hamiduzzaman, M.M.; Jakab, G.; Barnavon, L.; Neuhaus, J.M.; Mauch-Mani, B. β-Aminobutyric acid-induced resistance against downy mildew in grapevine acts through the potentiation of callose formation and jasmonic acid signaling. *Mol. Plant-Microbe Interact.* **2005**, *18*, 819–829. [CrossRef] [PubMed]
16. Wallis, C.M.; Chen, J. Grapevine phenolic compounds in xylem sap and tissues are significantly altered during infection by *Xylella Fastidiosa*. *Phytopathology* **2012**, *102*, 816–826. [CrossRef] [PubMed]
17. Tziros, G.T.; Ainalidou, A.; Samaras, A.; Kollaros, M.; Karamanoli, K.; Menkissoglu-Spiroudi, U.; Karaoglanidis, G.S. Differences in defence-related gene expression and metabolite accumulation reveal insights into the resistance of Greek grape wine cultivars to *Botrytis* bunch rot. *Oeno One* **2022**, *56*, 111–123. [CrossRef]
18. Perkins, M.L.; Schuetz, M.; Unda, F.; Chen, K.T.; Bally, M.B.; Kulkarni, J.A.; Yan, Y.; Pico, J.; Castellarin, S.D.; Mansfield, S.D.; et al. Monolignol export by diffusion down a polymerization-induced concentration gradient. *Plant Cell* **2022**, *34*, 2080–2095. [CrossRef] [PubMed]
19. Yu, Y. LACCASE2 negatively regulates lignin deposition of *Arabidopsis* Roots. *Plant Physiol.* **2020**, *182*, 1190–1191. [CrossRef] [PubMed]
20. Zhao, Q.; Nakashima, J.; Chen, F.; Yin, Y.; Fu, C.; Yun, J.; Shao, H.; Wang, X.; Wang, Z.-Y.; Dixon, R.A. LACCASE is necessary and nonredundant with PEROXIDASE for lignin polymerization during vascular development in *Arabidopsis*. *Plant Cell* **2013**, *25*, 3976–3987. [CrossRef] [PubMed]
21. Liang, M.; Davis, E.; Gardner, D.; Cai, X.; Wu, Y. Involvement of AtLAC15 in lignin synthesis in seeds and in root elongation of *Arabidopsis*. *Planta* **2006**, *224*, 1185–1196. [CrossRef] [PubMed]
22. Berthet, S.; Demont-Caulet, N.; Pollet, B.; Bidzinski, P.; Cezard, L.; Le Bris, P.; Borrega, N.; Herve, J.; Blondet, E.; Balzergue, S.; et al. Disruption of LACCASE4 and 17 results in tissue-specific alterations to lignification of *Arabidopsis thaliana* stems. *Plant Cell* **2011**, *23*, 1124–1137. [CrossRef] [PubMed]
23. Perkins, M.L.; Schuetz, M.; Unda, F.; Smith, R.A.; Sibout, R.; Hoffmann, N.J.; Wong, D.C.J.; Castellarin, S.D.; Mansfield, S.D.; Samuels, L. Dwarfism of high-monolignol *Arabidopsis* plants is rescued by ectopic *LACCASE* overexpression. *Plant Direct* **2020**, *4*, e00265. [CrossRef] [PubMed]
24. He, F.; Machemer-Noonan, K.; Golfier, P.; Unda, F.; Dechert, J.; Zhang, W.; Hoffmann, N.; Samuels, L.; Mansfield, S.D.; Rausch, T.; et al. The in vivo impact of MsLAC1, a *Miscanthus* laccase isoform, on lignification and lignin composition contrasts with its in vitro substrate preference. *BMC Plant Biol.* **2019**, *19*, 552. [CrossRef]
25. Xue, C.; Yao, J.-L.; Qin, M.-F.; Zhang, M.-Y.; Allan, A.C.; Wang, D.-F.; Wu, J. PbrmiR397a regulates lignification during stone cell development in pear fruit. *Plant Biotechnol. J.* **2019**, *17*, 103–117. [CrossRef] [PubMed]
26. Qin, S.; Fan, C.; Li, X.; Li, Y.; Hu, J.; Li, C.; Luo, K. LACCASE14 is required for the deposition of guaiacyl lignin and affects cell wall digestibility in poplar. *Biotechnol. Biofuels* **2020**, *13*, 197. [CrossRef] [PubMed]
27. Wang, X.; Zhuo, C.; Xiao, X.; Wang, X.; Docampo-Palacios, M.; Chen, F.; Dixon, R.A. Substrate specificity of LACCASE8 facilitates polymerization of caffeyl alcohol for C-lignin biosynthesis in the seed coat of *Cleome hassleriana*. *Plant Cell* **2020**, *32*, 3825–3845. [CrossRef] [PubMed]
28. Balasubramanian, V.K.; Rai, K.M.; Thu, S.W.; Hii, M.M.; Mendu, V. Genome-wide identification of multifunctional laccase gene family in cotton (*Gossypium* spp.); expression and biochemical analysis during fiber development. *Sci. Rep.* **2016**, *6*, 34309. [CrossRef] [PubMed]
29. Wei, T.; Tang, Y.; Jia, P.; Zeng, Y.; Wang, B.; Wu, P.; Quan, Y.; Chen, A.; Li, Y.; Wu, J. A Cotton lignin biosynthesis gene, *GhLAC4*, fine-tuned by Ghr-miR397 modulates plant resistance against *Verticillium dahliae*. *Front. Plant Sci.* **2021**, *12*, 743795. [CrossRef] [PubMed]
30. Zhang, Y.; Wu, L.; Wang, X.; Chen, B.; Zhao, J.; Cui, J.; Li, Z.; Yang, J.; Wu, L.; Wu, J.; et al. The cotton laccase gene *GhLAC15* enhances *Verticillium* wilt resistance via an increase in defence-induced lignification and lignin components in the cell walls of plants. *Mol. Plant Pathol.* **2019**, *20*, 309–322. [CrossRef] [PubMed]
31. Hu, Q.; Min, L.; Yang, X.; Jin, S.; Zhang, L.; Li, Y.; Ma, Y.; Qi, X.; Li, D.; Liu, H.; et al. Laccase GhLac1 modulates broad-spectrum biotic stress tolerance via manipulating phenylpropanoid pathway and jasmonic acid synthesis. *Plant Physiol.* **2018**, *176*, 1808–1823. [CrossRef] [PubMed]

32. Yu, X.; Gong, H.; Cao, L.; Hou, Y.; Qu, S. MicroRNA397b negatively regulates resistance of *Malus hupehensis* to *Botryosphaeria dothidea* by modulating *MhLAC7* involved in lignin biosynthesis. *Plant Sci.* **2020**, *292*, 110390. [CrossRef] [PubMed]
33. Hou, Y.; Yu, X.; Chen, W.; Zhuang, W.; Wang, S.; Sun, C.; Cao, L.; Zhou, T.; Qu, S. MdWRKY75e enhances resistance to *Alternaria alternata* in *Malus domestica*. *Hortic. Res.* **2021**, *8*, 225. [CrossRef] [PubMed]
34. Zhu, Y.; Li, G.; Singh, J.; Khan, A.; Fazio, G.; Saltzgiver, M.; Xia, R. Laccase directed lignification is one of the major processes associated with the defense response against *Pythium ultimum* infection in apple roots. *Front. Plant Sci.* **2021**, *12*, 629776. [CrossRef] [PubMed]
35. Zhao, Y.; Liu, Y.; Dong, X.; Liu, J.-J.; Zhao, D.-G. Identification of a novel laccase gene *EuLAC1* and its potential resistance against *Botrytis cinerea*. *Transgenic Res.* **2022**, *31*, 215–225. [CrossRef] [PubMed]
36. Wan, R.; Guo, C.; Hou, X.; Zhu, Y.; Gao, M.; Hu, X.; Zhang, S.; Jiao, C.; Guo, R.; Li, Z.; et al. Comparative transcriptomic analysis highlights contrasting levels of resistance of *Vitis vinifera* and *Vitis amurensis* to *Botrytis cinerea*. *Hortic. Res.* **2021**, *8*, 103. [CrossRef] [PubMed]
37. Kumar, S.; Stecher, G.; Li, M.; Knyaz, C.; Tamura, K. MEGA X: Molecular evolutionary genetics analysis across computing platforms. *Mol. Biol. Evol.* **2018**, *35*, 1547–1549. [CrossRef] [PubMed]
38. Letunic, I.; Bork, P. Interactive tree of life (iTOL) v3: An online tool for the display and annotation of phylogenetic and other trees. *Nucleic Acids Res.* **2016**, *44*, W242–W245. [CrossRef] [PubMed]
39. McCaig, B.C.; Meagher, R.B.; Dean, J.F.D. Gene structure and molecular analysis of the laccase-like multicopper oxidase (LMCO) gene family in *Arabidopsis thaliana*. *Planta* **2005**, *221*, 619–636. [CrossRef] [PubMed]
40. Liao, B.; Wang, C.; Li, X.; Man, Y.; Ruan, H.; Zhao, Y. Genome-wide analysis of the *Populus trichocarpa* laccase gene family and functional identification of PtrLAC23. *Front. Plant Sci.* **2023**, *13*, 1063813. [CrossRef]
41. Xu, X.; Zhou, Y.; Wang, B.; Ding, L.; Wang, Y.; Luo, L.; Zhang, Y.; Kong, W. Genome-wide identification and characterization of laccase gene family in *Citrus sinensis*. *Gene* **2019**, *689*, 114–123. [CrossRef] [PubMed]
42. Lescot, M.; Déhais, P.; Thijs, G.; Marchal, K.; Moreau, Y.; Van de Peer, Y.; Rouzé, P.; Rombauts, S. PlantCARE, a database of plant cis-acting regulatory elements and a portal to tools for in silico analysis of promoter sequences. *Nucleic Acids Res.* **2002**, *30*, 325–327. [CrossRef] [PubMed]
43. Shi, J.; Yao, J.; Tong, R.; Wang, S.; Li, M.; Song, C.; Wan, R.; Jiao, J.; Zheng, X. Genome-wide identification of laccase gene family from *Punica granatum* and functional analysis towards potential involvement in lignin biosynthesis. *Horticulturae* **2023**, *9*, 918. [CrossRef]
44. Zhu, J.; Zhang, H.; Huang, K.; Guo, R.; Zhao, J.; Xie, H.; Zhu, J.; Gu, H.; Chen, H.; Li, G.; et al. Comprehensive analysis of the laccase gene family in tea plant highlights its roles in development and stress responses. *BMC Plant Biol.* **2023**, *23*, 129. [CrossRef] [PubMed]
45. Wan, R.; Song, J.; Lv, Z.; Qi, X.; Han, X.; Guo, Q.; Wang, S.; Shi, J.; Jian, Z.; Hu, Q.; et al. Genome-wide identification and comprehensive analysis of the *AP2/ERF* gene family in pomegranate fruit development and postharvest preservation. *Genes* **2022**, *13*, 895. [CrossRef]
46. Mayolo-Deloisa, K.; Gonzalez-Gonzalez, M.; Rito-Palomares, M. Laccases in food industry: Bioprocessing, potential industrial and biotechnological applications. *Front. Bioeng. Biotechnol.* **2020**, *8*, 222. [CrossRef] [PubMed]
47. Cai, X.; Davis, E.J.; Ballif, J.; Liang, M.; Bushman, E.; Haroldsen, V.; Torabinejad, J.; Wu, Y. Mutant identification and characterization of the laccase gene family in *Arabidopsis*. *J. Exp. Bot.* **2006**, *57*, 2563–2569. [CrossRef] [PubMed]
48. Liu, Q.; Luo, L.; Wang, X.; Shen, Z.; Zheng, L. Comprehensive Analysis of Rice Laccase Gene (OsLAC) Family and ectopic expression of *OsLAC10* enhances tolerance to copper stress in *Arabidopsis*. *Int. J. Mol. Sci.* **2017**, *18*, 209. [CrossRef] [PubMed]
49. Wen, J.; Liu, Y.; Yang, S.; Yang, Y.; Wang, C. Genome-wide characterization of laccase gene family from turnip and chinese cabbage and the role in xylem lignification in hypocotyls. *Horticulturae* **2022**, *8*, 522. [CrossRef]
50. Sun, Z.; Zhou, Y.; Hu, Y.; Jiang, N.; Hu, S.; Li, L.; Li, T. Identification of wheat LACCASEs in response to *Fusarium graminearum* as potential deoxynivalenol trappers. *Front. Plant Sci.* **2022**, *13*, 832800. [CrossRef] [PubMed]
51. Ramirez, V.; Garcia-Andrade, J.; Vera, P. Enhanced disease resistance to Botrytis cinerea in myb46 *Arabidopsis* plants is associated to an early down-regulation of *CesA* genes. *Plant Signal. Behav.* **2011**, *6*, 911–913. [CrossRef] [PubMed]
52. Wang, Y.; Xin, H.; Fan, P.; Zhang, J.; Liu, Y.; Dong, Y.; Wang, Z.; Yang, Y.; Zhang, Q.; Ming, Y.; et al. The genome of Shanputao (*Vitis amurensis*) provides a new insight into cold tolerance of grapevine. *Plant Fournal* **2021**, *105*, 1495–1506. [CrossRef] [PubMed]
53. Zhu, Y.; Zhang, X.; Zhang, Q.; Chai, S.; Yin, W.; Gao, M.; Li, Z.; Wang, X. The transcription factors *VaERF16* and *VaMYB306* interact to enhance resistance of grapevine to *Botrytis cinerea* infection. *Mol. Plant Pathol.* **2022**, *23*, 1415–1432. [CrossRef] [PubMed]
54. Wang, M.; Zhu, Y.; Han, R.; Yin, W.; Guo, C.; Li, Z.; Wang, X. Expression of *Vitis amurensis* VaERF20 in *Arabidopsis thaliana* improves resistance to *Botrytis cinerea* and *Pseudomonas syringae* pv. tomato DC3000. *Int. J. Mol. Sci.* **2018**, *19*, 696. [CrossRef] [PubMed]
55. Zhou, J.; Lee, C.; Zhong, R.; Ye, Z. MYB58 and MYB63 are transcriptional activators of the lignin biosynthetic pathway during secondary cell wall formation in *Arabidopsis*. *Plant Cell* **2009**, *21*, 248–266. [CrossRef] [PubMed]
56. Fu, J.; Huang, S.; Qian, J.; Qing, H.; Wan, Z.; Cheng, H.; Zhang, C. Genome-Wide identification of *Petunia HSF* genes and potential function of *PhHSF19* in benzenoid/phenylpropanoid biosynthesis. *Int. J. Mol. Sci.* **2022**, *23*, 2974. [CrossRef] [PubMed]
57. Schmitt, A.P.; McEntee, K. Msn2p, a zinc finger DNA-binding protein, is the transcriptional activator of the multistress response in *Saccharomyces cerevisiae*. *Proc. Natl. Acad. Sci. USA* **1996**, *93*, 5777–5782. [CrossRef] [PubMed]